

# Diffusion of Sticky Nanoparticles in a Polymer Melt: Crossover from Suppressed to Enhanced Transport

Bobby Carroll,<sup>†</sup> Vera Bocharova,<sup>\*,§</sup> Jan-Michael Y. Carrillo,<sup>||</sup> Alexander Kisiuk,<sup>§</sup> Shiwang Cheng,<sup>⊥</sup> Umi Yamamoto,<sup>#</sup> Kenneth S. Schweizer,<sup>¶</sup> Bobby G. Sumpter,<sup>||</sup> and Alexei P. Sokolov<sup>\*,†,‡,§</sup>

<sup>†</sup>Department of Physics and Astronomy and <sup>‡</sup>Department of Chemistry, University of Tennessee, Knoxville, Tennessee 37996, United States

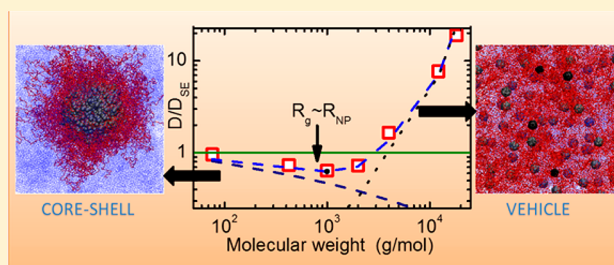
<sup>§</sup>Chemical Sciences Division and <sup>||</sup>Center for Nanophase Materials Sciences and Computational Sciences & Engineering Division, Oak Ridge National Laboratory, Oak Ridge, Tennessee 37831, United States

<sup>⊥</sup>Department of Chemical Engineering and Materials Science, Michigan State University, East Lansing, Michigan 48824, United States

<sup>#</sup>Division of Chemistry and Chemical Engineering, California Institute of Technology, Pasadena, California 91125, United States

<sup>¶</sup>Departments of Materials Science and Chemistry, Frederick Seitz Materials Research Laboratory, University of Illinois, Urbana, Illinois 61801, United States

**ABSTRACT:** The self-diffusion of a single large particle in a fluid is usually described by the classic Stokes–Einstein (SE) hydrodynamic relation. However, there are many fluids where the SE prediction for nanoparticles diffusion fails. These systems include diffusion of nanoparticles in porous media, in entangled and unentangled polymer melts and solutions, and protein diffusion in biological environments. A fundamental understanding of the microscopic parameters that govern nanoparticle diffusion is relevant to a wide range of applications. In this work, we present experimental measurements of the tracer diffusion coefficient of small and large nanoparticles that experience strong attractions with unentangled and entangled polymer melt matrices. For the small nanoparticle system, a crossover from suppressed to enhanced diffusion is observed with increasing polymer molecular weight. We interpret these observations based on our theoretical and simulation insights of the preceding article (paper 1) as a result of a crossover from an effective hydrodynamic core–shell to a nonhydrodynamic vehicle mechanism of transport, with the latter strongly dependent on polymer–nanoparticle desorption time. A general zeroth-order qualitative picture for small sticky nanoparticle diffusion in polymer melts is proposed.



## I. INTRODUCTION

This article (paper 2) presents and interprets new experimental measurements of the influence of strong particle–polymer attractions on nanoparticle diffusion and is a companion to the preceding purely theory/simulation paper 1.<sup>1</sup> An overview of the study of nanoparticle motion for experimental,<sup>2–13</sup> theoretical,<sup>14–20</sup> and simulation<sup>21,22</sup> studies was given in paper 1. Current theories go far beyond a simplified free volume approach based essentially on geometrical arguments (see e.g. ref 23). Further, the relevance of this problem to critical technologies (e.g., processing of nanocomposite materials,<sup>9,22,24</sup> filtration and purification systems,<sup>25,26</sup> catalysis,<sup>27</sup> drug delivery,<sup>28,29</sup> and other biological processes such as protein diffusion<sup>30–32</sup>) was also emphasized. The continuum hydrodynamic description of nanoparticle (NP) diffusion in a simple liquid is based on the Stokes–Einstein (SE) relation, which for static boundary conditions is

$$D_{SE} = \frac{k_B T}{6\pi\eta R} \quad (1)$$

where  $R$  is the nanoparticle (NP) radius and  $\eta$  is the liquid medium shear viscosity.<sup>33</sup> Equation 1 assumes the diffusing particle is larger than all relevant structural and dynamic length scales of the matrix and moves slower compared to any relaxation times of the suspending liquid. However, many recent experimental studies have revealed strong deviations from the SE prediction for biological systems,<sup>30,32,34</sup> polymer solutions,<sup>35,36</sup> and polymer melts.<sup>2,3,8,11</sup>

In polymer melts, the important parameters are the polymer radius of gyration ( $R_g$ ), segment size, and (if entangled) the polymer tube diameter  $d_T$ . The interplay between these parameters determines the characteristic dynamical regimes that describe polymer relaxation on different length scales spanning the range from segment size to coil size. A crucial energy scale is set by the polymer–nanoparticle interaction. For repulsive (“nonsticky”) nanoparticles, huge SE violations

Received: December 19, 2017

Revised: February 14, 2018

Published: March 9, 2018

**Table 1. Results for OAPS and SiO<sub>2</sub> Nanoparticles Diffusion in PPG Melts<sup>a</sup>**

name	$M_w$	PDI	$\eta$ (Pa·s)	decay $\tau$ (s)	$R_g$ (nm)	$D$ (m <sup>2</sup> /s)	$D_{SE}$ (m <sup>2</sup> /s)	$D/D_{SE}$	$N/N_e$
OAPS									
1	76 (PG)	1	0.04322	$4.60 \times 10^{-4}$		$5.39 \times 10^{-12}$	$5.61 \times 10^{-12}$		0.026
2	425	1.27	0.134	0.00181	0.65	$1.34 \times 10^{-12}$	$1.81 \times 10^{-12}$	0.74	0.15
3	1000	1.12	0.18662	0.00291	0.99	$8.31 \times 10^{-13}$	$1.30 \times 10^{-12}$	0.64	0.35
4	2000	1.05	0.385	0.00524	1.41	$4.61 \times 10^{-13}$	$6.29 \times 10^{-13}$	0.73	0.71
5	4000	1.03	1.25172	0.00751	1.99	$3.21 \times 10^{-13}$	$1.94 \times 10^{-13}$	1.66	1.41
6	12200		8.05	0.01042	3.47	$2.31 \times 10^{-13}$	$3.01 \times 10^{-14}$	7.68	4.31
7	18200		28.5	0.01494	4.24	$1.61 \times 10^{-13}$	$8.50 \times 10^{-15}$	18.92	6.43
SiO <sub>2</sub>									
1	76 (PG)	1	0.04322	0.00253		$9.81 \times 10^{-13}$	$9.87 \times 10^{-13}$		0.026
2	425	1.27	0.134	0.0079	0.65	$3.07 \times 10^{-13}$	$3.18 \times 10^{-13}$	0.96	0.15
3	1000	1.12	0.18662	0.0116	0.99	$2.09 \times 10^{-13}$	$2.29 \times 10^{-13}$	0.91	0.35
4	2000	1.05	0.30898	0.02034	1.41	$1.06 \times 10^{-13}$	$1.38 \times 10^{-13}$	0.77	0.71
5	4000	1.03	1.25172	0.102	1.99	$2.37 \times 10^{-14}$	$3.41 \times 10^{-14}$	0.70	1.41

<sup>a</sup>Molecular weight  $M_w$ , polydispersity index (PDI), shear viscosity  $\eta$ , dynamic light scattering relaxation time  $\tau$ , chain radius of gyration  $R_g$  based on characteristic ratio  $C_\infty = 5.1$ ,<sup>38</sup> nanoparticle (NP) diffusion constant  $D$ , the expected value of  $D_{SE}$  using the bare NP radius, the ratio of NP to SE diffusivities  $D/D_{SE}$ , and the number of entanglements  $N/N_e$  assuming a molecular weight between entanglements of  $M_e = 2832$ .<sup>38</sup> The PPG tube diameter  $d_T = 4.9$  nm.<sup>38</sup>

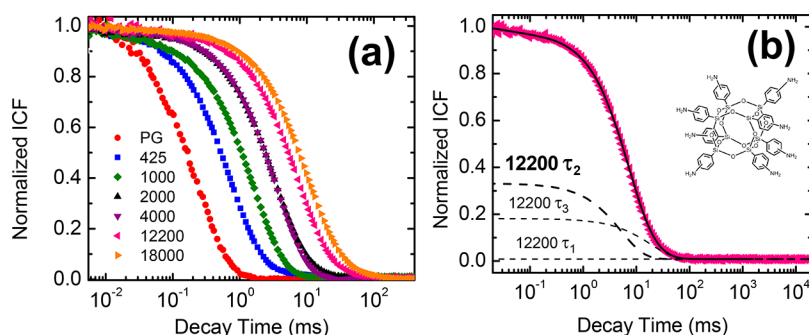


**Figure 1.** (a) Intensity correlation functions for OAPS particles in PPG of molecular weights shown by numbers in g/mol. (b) An example of the intensity correlation function for the OAPS in PPG with MW = 12 200 g/mol sample (symbols) and its fit by a three-exponential decay function (solid line). Dashed lines show three processes separately. The  $\tau_2$  decay functions are taken to be the single particle diffusion.

(diffusion much faster than predicted by  $D_{SE}$ ) were reported for NPs smaller than the  $d_T$ ,<sup>2,3</sup> which can persist to particle diameters well beyond the entanglement length scale. For unentangled polymers, faster than SE diffusion occurs when  $R < R_g$ . Multiple theoretical<sup>15,16,18,19</sup> and simulation<sup>21,22</sup> studies have been performed for repulsive nanoparticles in polymer melts and solutions, and the problem seems rather well understood.

On the other hand, understanding NP diffusion for the case of strongly attractive (“sticky”) polymer–nanoparticle interactions is more complicated and less understood. These systems, however, are of great interest because attractive interactions are required for good nanoparticle solubility and dispersion in polymer nanocomposites.<sup>17,24</sup> Here an additional crucial and material-specific parameter affecting diffusion enters: the polymer–NP desorption time,  $\tau_{des}$ . For instance, if polymers remain adsorbed to the NP for a sufficiently long time, they should slow down NP diffusion in ways not previously reported. A recent experimental study of a sticky NP larger than both  $d_T$  and  $R_g$  revealed<sup>37</sup> a suppressed (slower than  $D_{SE}$ , eq 1) diffusion that can be described by assuming an effective hydrodynamic “core–shell” mechanism, where eq 1 applies but with an effective particle radius,  $R_{eff} \sim R + R_g$ ,<sup>37</sup> larger than the nominal nanoparticle size  $R$ . However, as discussed in paper 1, for small “sticky” NPs with  $R < d_T$  or  $R_g$ , another NP diffusion mechanism may become important—the

“vehicle” mechanism where adsorbed small particles use polymer chains as carriers or “vehicles”. Multiple different NP diffusion regimes can exist when  $\tau_{des}$  is shorter than other characteristic time scales in the polymer liquid, as discussed in ref 1.

In this article we experimentally measure the diffusion constant of silica nanoparticles ( $R = 5$  nm) and octaamino-phenylsilsequioxane (OAPS) nanoparticles ( $R = 0.88$  nm) in polypropylene glycol (PPG) melts of different molecular weights (MWs). We find that over the entire studied MW range silica NPs diffuse slower than predicted by the SE relation. In contrast, OAPS nanoparticles diffuse slower than the SE prediction only in short chain polymer melts; at larger MW there is a crossover to much faster diffusion than SE. The crossover from suppressed to enhanced diffusion occurs for this specific system when  $R_g \sim R$ . We apply the theoretical and simulation insights of paper 1 to demonstrate that this unusual behavior is caused by a finite  $\tau_{des}$  for the OAPS–PPG system. To leading order, the observed nonmonotonic variation of the ratio  $D_{NP}/D_{SE}$  with PPG molecular weight can be qualitatively described by a crossover from an effective hydrodynamic core–shell mechanism of transport to a vehicle type of diffusion, with the latter strongly dependent on the chemically specific value of  $\tau_{des}$ . On the basis of the results of paper 1 and the current paper, we offer a qualitative general scenario for the diffusion of sticky and repulsive nanoparticles in polymer melts.

The remainder of the article is structured as follows. Section II describes the experimental materials and methods, while section III presents the experimental nanoparticle diffusion data and its analysis. Section IV briefly summarizes the simulations and theory methods from paper 1, which are then employed to interpret the experimental results in section V. Based on the combined theoretical and experimental results, section VI formulates a qualitative general picture for the diffusion of nanoparticles in a polymer melt or solution with attractive or repulsive interactions. Section VII presents our conclusions.

## II. EXPERIMENTAL MATERIALS AND METHODS

Polypropylene glycol (PPG) of varying molecular weight (76, 425, 1000, 2000, and 4000 g/mol), tetrahydrofuran (THF), and methyl ethyl ketone (MEK) were purchased from Sigma-Aldrich and used as received. The polydispersity index (PDI) of the polymers was estimated from gel permeation chromatography (GPC) (Table 1). Additional PPG of MW 12 200 and 18 200 g/mol were obtained from Catalin Gainaru (TU Dortmund). Two different nanoparticles were used: silica (SiO<sub>2</sub>) particles ( $R = 5 \pm 1.3$  nm, purchased from Nissan Chemicals) and OAPS ( $R = 0.88 \pm 0.002$  nm, purchased from Mayaterials; with the chemical structure is shown in the Figure 1 inset). The distribution of silica nanoparticles sizes was estimated in MEK solution using dynamic light scattering (DLS). Both nanoparticles form hydrogen bonds with PPG and can be considered as “sticky”. For SiO<sub>2</sub> NPs, the hydrogen bonds are formed by hydroxyl groups, while OAPS particles form H-bonds via amino groups.

Samples were made by first dissolving PPG (4 g) in THF in a glass vial under stirring conditions (concentration of 1 g/mL) for mixing with OAPS and in MEK for mixing with SiO<sub>2</sub>. The solutions were added to the corresponding PPG solutions dropwise and stirred for 20 min. Afterwards, the cap was removed from the vial, and the solvent was allowed to evaporate overnight under stirring at room temperature. To remove any residual solvent, the samples were vacuum-dried for 24 h at room temperature with an Isotemp Model 280A (Fisher Scientific) vacuum oven and turbo pump that created a vacuum of  $10^{-6}$  mbar. After drying, the PPG/OAPS and PPG/SiO<sub>2</sub> samples were filtered using a 0.02  $\mu\text{m}$  Anotop and 0.1  $\mu\text{m}$  PTFE syringe filter, respectively, using a custom-built filtering device. The final concentration of nanoparticles did not exceed  $\sim 1$  wt % ( $\sim 0.7$  vol %) for PPG/OAPS samples. For SiO<sub>2</sub>, the concentration was significantly lower than  $\sim 1$  wt % to avoid nanoparticle aggregation. Residual SiO<sub>2</sub> NPs aggregation prevented measurements for PPG with higher MWs (12 200 and 18 200 g/mol).

Dynamic light scattering (DLS) was employed to measure the translational diffusion constant of nanoparticles in PPG melts at 291 K. A HeNe laser (Newport R-31425, 632.8 nm, 35 mW) with vertically polarized light passing through the sample was employed. Scattered light was collected at 90°, passed through an analyzer (VV polarization), and filtered using Semrock 632.8 nm MaxLine cleanup filter to suppress Raman and fluorescent signals from the sample. The filtered light was collected by an ALV static and dynamic enhancer and passed through a beam splitter which divided it into two equal light signals that are detected by two avalanche photodiodes (Pacer SPCM-AQRH-14-FC). A cross-correlation function of the signals was measured using a ALV-7004 digital correlator.

Rheological measurements on neat PPG, PPG/OAPS, and PPG/SiO<sub>2</sub> were performed on an AR-2000ex rheometer (TA Instruments) with a cone–plane geometry in an environmental chamber. The cone has a diameter of 25 mm, a cone angle of 2°, and 58  $\mu\text{m}$  in truncation. Viscosities were measured at  $T = 291$  K in flow mode at a continuous shear rate of  $10$  s<sup>-1</sup>. The viscosities of the two composite systems were the same as in the neat polymers, and their values are listed in Table 1.

## III. EXPERIMENTAL RESULTS

Figure 1a presents intensity correlation function (ICF) DLS data for each molecular weight for the PPG/OAPS system. An example of a fit is given in Figure 1b. In many cases a single-

exponential function fits the data well. However, a weaker second process was evident in some spectra (Figure 1b) that is probably related to some degree of NP aggregation. In several cases a third, faster process was needed to fit the data, which we believe is of polymer origin. Thus, in general the measured correlation functions were fit with three-exponential decay functions:

$$g_1(t) = [A_1 e^{-t/\tau_1} + A_2 e^{-t/\tau_2} + A_3 e^{-t/\tau_3}]^2 + \text{constant } t \quad (2)$$

Despite the presence of possibly three processes (Figure 1b), the main second process always has a higher amplitude and can be clearly distinguished as reflecting translational Fickian diffusion.

The NP diffusion constant was determined using

$$D_{\text{NP}} = \frac{1}{q^2 \tau_2}, \quad q = \frac{4\pi n}{\lambda} \sin\left(\frac{\theta}{2}\right) \quad (3)$$

where  $q$  is the scattering wave vector and  $\theta$  is the scattering angle, which is 90° for this setup.

The SiO<sub>2</sub> and OAPS diffusion constants obtained from eqs 3 are shown in Figure 2 as a function of PPG MW. Interestingly,

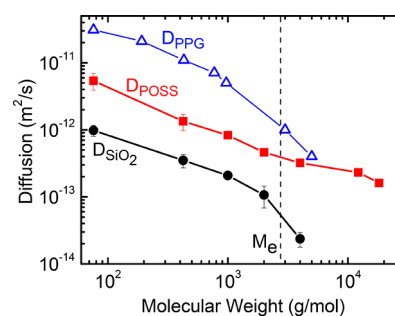


**Figure 2.** Diffusion constant for OAPS (red squares) and SiO<sub>2</sub> (black circles) nanoparticles as a function of PPG melt molecular weight. The CM diffusion constant of PPG chains (blue triangles) from ref 39 is presented for comparison. The error bars for PPG diffusion are not known. The error bars for the nanoparticle diffusion that are not visible are of the order of the symbol size. Dashed line marks entanglement MW,  $M_e = 2832$  g/mol.<sup>38</sup>

the polymer chain length dependences for diffusion of both NPs are similar at low MW and roughly follow a power law decrease with an apparent exponent less than unity. Plausibly, the latter reflects the sublinear MW growth of the unentangled PPG melt viscosity we have measured (see Table 1). As the MW approaches and then exceeds the entanglement MW,  $M_e$ , the SiO<sub>2</sub> diffusivity appears to begin diverging from the POSS diffusivity, albeit for only one data point available above  $M_e$ . The same behavior was also reported for a different polymer–nanoparticle system<sup>37</sup> with attractive interaction and comparable size of SiO<sub>2</sub> nanoparticles on the wider range of molecular weights. The decrease of the SiO<sub>2</sub> NP diffusion constant does become significantly steeper as  $M > M_e$  in qualitative contrast to the modest but clear weakening behavior seen for the OAPS diffusion constant. We note that at low MW the center-of-mass (CM) diffusion constant of PPG chains in the melt is faster than that of OAPS particles, but they become comparable at  $MW \sim 6000 \sim 2M_e$  (Figure 2).

#### IV. SIMULATION AND THEORY METHODS

Physical interpretation of the experimental data is based on the integrated theory and simulation study of paper 1. Here we briefly summarize the findings relevant to the present measurements.

**A. MD Simulations.** The coarse-grained MD simulation results of paper 1 chose model parameters to mimic the OAPS–PPG system with different chain length  $N$ . Figure 3

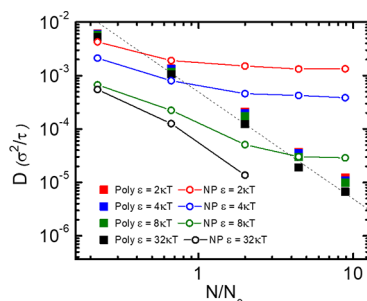


**Figure 3.** MD simulation results (open symbols + lines) for the diffusion constant of small “sticky” NPs with different strength of NP–polymer interactions  $\epsilon$  in polymer melts with different chain length  $N$  scaled by the entanglement value  $N_e$  ( $N_e = 45$ ). The chain CM diffusion constant is also presented (filled symbols), and the dashed line shows the expected entangled behavior  $\sim M^{-2}$ . Although initially NP diffusion is slower than chain diffusion, it becomes faster above a characteristic chain length, and this crossover depends on the strength of NP–polymer interactions.

presents the NP diffusion constants over a large range of  $N/N_e$  ( $N_e = 45$  is the chain length between entanglements<sup>1</sup>) for various strengths of segment–NP attraction ( $\epsilon \sim 2\text{--}32 k_B T$ ). The latter provides wide tuning of the segmental desorption time  $\tau_{\text{des}}$ . The NP diffusion in a melt of short chains is slower than chain diffusion, and the slowing down increases with attractive interaction strength. Such behavior is explained as a result of slowing down of segmental dynamics in the interfacial polymer layer with an increase of polymer–NP attraction.<sup>24</sup> The NP diffusivity in simulation saturates at higher  $N$ , in contrast to the chain CM diffusivity which decreases strongly at higher  $N$ . For weaker polymer–NP attraction ( $\sim 2\text{--}4 k_B T$ ), the NP diffusion constant becomes  $N$ -independent at a relatively low  $N/N_e < 1\text{--}2$ . For stronger polymer–NP attraction ( $8 k_B T$ ), the saturation chain length grows to  $N/N_e \sim 4$ .

**B. Density Functional Theory.** In an attempt to relate our coarse-grained MD simulations to the OAPS–PPG system of interest, spin-polarized density functional theory (DFT) calculations were performed using the VASP package.<sup>40</sup> The Kohn–Sham equations were solved using the projector augmented wave (PAW) approach and a plane-wave basis with a 400 eV energy cutoff. The exchange–correlation interactions were considered in the generalized gradient approximation (GGA) using the Perdew–Burke–Ernzerhof (PBE) functional.<sup>41</sup> To account for nonlocal correlations (dispersion interactions), we used the vdW-DF2 approach.<sup>42</sup> Electronic convergence was defined as a consistency between successive cycles of less than  $10^{-5}$  eV. Supercells consisting of OAPS (124 atoms) and a monomer of PPG (12 atoms) with a vacuum layer of at least 18 Å were used to avoid spurious interactions with periodic images. Full relaxation (geometry optimization) was performed with a K-point sampling restricted to the Gamma point, which is appropriate for the finite cluster

calculations performed here. All atoms were relaxed until the residual forces were below 0.01 eV/Å. The OAPS–monomer interaction energies were then determined by computing the difference between the total energy of the cluster (OAPS–PPG) and the individual molecular constituents. These DFT calculations suggest the effective monomer–OAPS attraction energy is  $\sim 15$  kJ/mol, or  $\sim 6 k_B T$  at  $T = 291$  K.

**C. Simplified Theory.** Paper 1<sup>1</sup> presented an in-depth discussion of a theoretical approach for sticky NP diffusion based on competing core–shell and vehicle transport mechanisms. Detailed comparisons with MD simulations qualitatively support the general picture constructed. The theory predicts that the diffusion of a sticky NP can be described as a sum of two competing diffusion mechanisms:

$$D_{\text{NP}} = D_{\text{core-shell}} + D_{\text{vehicle}} \quad (4)$$

In the limiting regime of  $R > R_g$ ,  $D_{\text{core-shell}}$  should dominate, corresponding to an effective SE diffusion of the NP with  $R_{\text{eff}} \sim R + R_g$ . For  $R_g \gg R$ , the vehicle mechanism is dominant where polymers serve as a carrier of adsorbed nanoparticles. The former mechanism leads to a NP diffusivity that decreases with polymer MW, while the latter mechanism becomes MW-independent for long enough chains if the desorption time is less than the Rouse time. If the desorption time lies in between the Rouse and reptation times, a weak decrease with MW is predicted ( $D_{\text{vehicle}} \sim MW^{-1/2}$ ). All details can be found in paper 1.

Given the limited amount of experimental data, and the uncertainty concerning the desorption time for SiO<sub>2</sub> and OAPS nanoparticles in PPG melts, we employ a minimalist version of the theory to construct a simple, single adjustable parameter function:

$$D_{\text{NP}} = D_{\text{core-shell}} + D_{\text{vehicle}} = \frac{k_B T}{6\pi\eta R_{\text{eff}}} + AD_0 \quad (5)$$

The core–shell mechanism involves the full polymer melt viscosity and an effective NP radius, while vehicle mechanism is quantified by the segmental diffusion constant,  $D_0$ , and a dimensionless parameter,  $A$ , which is related to the desorption time and relevant polymer melt time scale.

#### V. INTERPRETATION OF EXPERIMENTAL OBSERVATIONS

We now discuss the experimental results of Figure 2 in more detail and present a minimalist analysis inspired by the theoretical and simulation results of paper 1. We begin with SiO<sub>2</sub> NP diffusion in PPG melts. The NP hydrodynamic radius measured in MEK solvent is  $R = 5.0 \pm 1.3$  nm, which corresponds to a diameter that is about twice larger than the tube diameter of PPG  $d_T \sim 4.9$  nm.<sup>38</sup> In our study, the  $R_g$  of the largest molecular weight PPG (MW = 4000 g/mol) we were able to dissolve SiO<sub>2</sub> NPs is  $R_g \sim 2$  nm (Table 1), which is smaller than  $R$ . The diffusion of SiO<sub>2</sub> NPs is observed to be slower than expected from the SE relationship, corresponding to a ratio  $D/D_{\text{SE}} < 1$  which decreases with PPG MW (Figure 4a). Similar behavior was reported by Griffin et al. for the diffusion of SiO<sub>2</sub> nanoparticles with  $R = 13$  nm in a poly(2-vinylpyridine) (P2VP) melt of different molecular weights.<sup>37</sup> Following the ideas presented in ref 37 and paper 1, Figure 4a shows that our observations are well described by the core–shell model (just the first term in eq 5) where the NP has a larger radius due to a so-called “bound” (on the NP diffusion

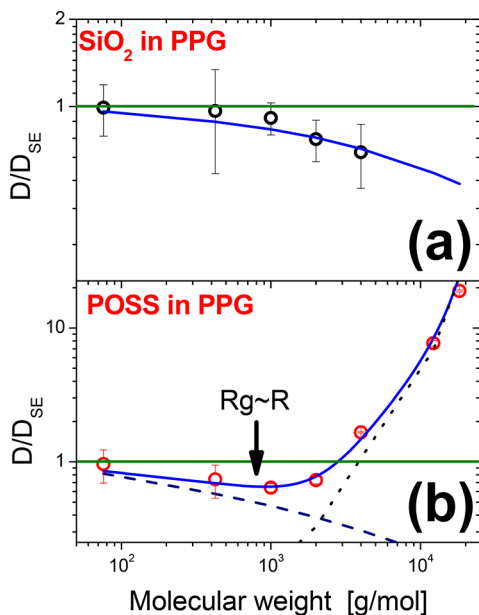


**Figure 4.** (a) Diffusion of SiO<sub>2</sub> NPs in PPG melts scaled by  $D_{SE}$  (symbols) vs MW of the polymer chains. The solid curve is the prediction of the core–shell mechanism with  $R_{eff} = R + R_g$ . (b) Diffusion of the OAPS particle in PPG melts scaled by  $D_{SE}$  (symbols) vs MW of the polymer chains. The black dashed curve is the prediction of the core–shell model with  $R_{eff} = R + R_g$ , while the black dotted curve corresponds to the diffusion constant (MW independent) predicted by the vehicle mechanism for relatively short  $\tau_{des}$ . The solid blue curve is the sum of these two diffusion coefficients. The arrow marks the molecular weight when  $R_g \sim R_{OAPS} \sim 0.9$  nm. The error bars are of the order of the symbol size for the points where they are not visible.

time scale) polymer layer of thickness  $\sim R_g$ . Such limiting behavior is expected to be applicable to entangled<sup>37</sup> and unentangled (our case here) systems as long as  $R > R_g$  and the NP desorption time exceeds the time scale for the onset of NP Fickian diffusion.<sup>1</sup> The chain desorption time from large attractive NPs is expected to be rather long due to multiple segments' adsorption from the same chain to their surface.

Qualitatively different behavior is observed for OAPS diffusion which has  $R = 0.88 \pm 0.002$  nm<sup>43</sup> (Figure 4b). At low MW it also shows suppressed diffusion that follows the same idea of renormalized hydrodynamic transport with an effectively larger radius  $R_{eff} \sim R + R_g$ . However, the  $D/D_{SE}$  goes through a minimum and crosses over to an enhanced (relative to the SE prediction) diffusion regime where it increases sharply with increasing polymer MW, reaching a factor of  $\sim 20$  larger than its hydrodynamic value (Figure 4b). According to the theory,<sup>1</sup> such enhanced diffusion is expected for small “sticky” NPs resulting from the vehicle mechanism of transport (eq 5). This mechanism predicts either constant or weakly MW-dependent NP diffusion for relatively short segmental desorption time. Assuming this term to be independent of MW, corresponding to the assumption that  $\tau_{des} < \tau_R$  (Rouse time), the NP diffusion (eq 5) scaled by the expected SE diffusion can be written as

$$\frac{D_{NP}}{D_{SE}} \approx \frac{1}{1 + \frac{R_g}{R}} + \frac{\eta}{\eta_0} B \quad (6)$$

The vehicle mechanism contribution (second term) contains the ratio of the full polymer melt viscosity  $\eta$  to its segmental

analogue  $\eta_0$ , and the parameter  $B$ , as discussed in paper 1, involves system-specific factors (including NP radius, polymer segment size, tube diameter, desorption time, and relevant polymer relaxation time). However, for a fixed NP and polymer system with  $\tau_{des} < \tau_R$  the parameter  $B$  is independent of the polymer MW, which results in a  $N$ -independent NP diffusivity in agreement with the simulations results at higher MW (Figure 3).

Although the OAPS diffusion constant does not reach the MW independent regime (Figure 2), by assuming  $D_{vehicle} = \text{constant} \sim 2 \times 10^{-13}$  m<sup>2</sup>/s (or the corresponding parameter  $B/\eta_0$  in eq 6), we find a very good description of the OAPS diffusion over the entire range of studied PPG molecular weights (Figure 4b). Assuming a weak MW dependence of  $D_{vehicle}$  per the theoretical analysis of paper 1 might further improve the agreement. Quantitatively, the apparent crossover between the core–shell and vehicle regimes occurs for this system at  $R_g \sim R$  (Figure 4b). Physically, an  $R_g$  of order or larger than  $R$  is necessary for the vehicle mechanism to be relevant, but the empirically defined crossover (Figure 4b) here is not a universal value of  $R_g/R$  and is strongly affected by  $\tau_{des}$ .

The MD simulations (Figure 3) found a  $N$ -independent regime for small “sticky” NP diffusion that shifts to higher  $N$  with an increase in segment–NP attractions and thus increase of  $\tau_{des}$ . Unfortunately, our experimental data do not provide a direct estimate of  $\tau_{des}$  for OAPS in PPG. However, some inferences can be made from comparisons of experiment with simulation and theory. We first note that the center-of-mass diffusion of nonadsorbed PPG chains should be faster than or comparable to the diffusion of a NP adsorbed to the chain. However, if the chain desorption time is shorter than the chain reptation time,  $\tau_{des} < \tau_{rep}$ , the diffusion of small ( $R < R_g$ ) NPs should become faster than chain diffusion.<sup>1</sup> Indeed, we do find that the OAPS diffusion is significantly slower than PPG chain diffusion at small MW and becomes comparable at a MW  $\sim 6000$  (Figure 2). The latter corresponds to MW  $\sim 2M_e$  for PPG, i.e., to  $N/N_e \sim 2$  in our simulations.<sup>1</sup> Chain and NP diffusion become comparable in our simulations at  $N/N_e \sim 0.7$  for  $\epsilon \sim 4 k_B T$  and at  $N/N_e \sim 4.4$  for  $\epsilon \sim 8 k_B T$  (Figure 3). By comparing experiment and simulation, we deduce the OAPS diffusion constant in PPG should correspond to  $\epsilon \sim 6 k_B T \sim 15$  kJ/mol (at  $T = 291$  K). Significantly, this estimate is consistent with our DFT calculations and suggests that an OAPS particle has one hydrogen bond per adsorbed PPG molecule. In that case the chain desorption time can be estimated as  $\tau_{des} \sim \tau_{seg} \exp(6) \sim 400 \tau_{seg}$  ( $\tau_{seg}$  is the segmental relaxation time of PPG chain). Analysis of dielectric spectroscopy data for PPG<sup>39</sup> reveals that segmental and chain relaxation time are separated by more than 3 orders for MW  $\sim 5500$  g/mol. This separation is consistent with the proposed scenario of vehicle diffusion when  $\tau_{des} < \tau_{rep}$  and likely also when  $\tau_{des} < \tau_R$ .

## VI. BROADER PICTURE

Constructing a broader theoretical picture that unifies the understanding of repulsive and sticky NPs in unentangled and entangled polymer melts and solutions requires more work. Beyond the obvious prefactor and other quantitative issues that enter a theoretical analysis, modeling the role of additional time and length scales in the crossover regime that bridges a pure core–shell type of diffusion (including both hydrodynamic and nonhydrodynamic effects per paper 1) to a vehicle type of diffusion is a challenging problem. The idea of an “effective NP diameter” is simple and attractive, but it is hard to defend in a

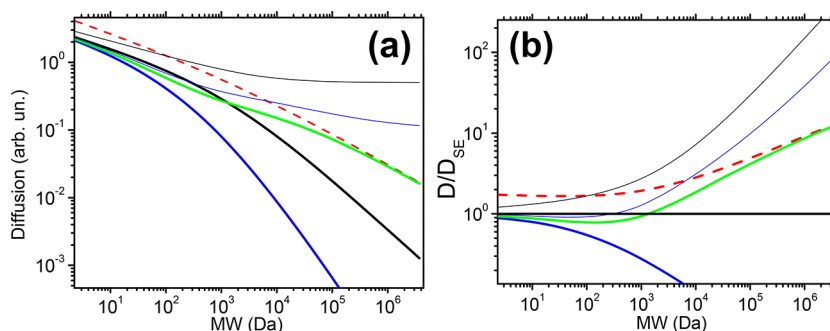


**Figure 5.** (a) Schematic presentation for various regimes of nanoparticle diffusion vs polymer  $R_g$  (i.e., molecular weight) in concentrated polymer solutions and melts. For nonadsorbing chains one has standard SE behavior (thick black line) for  $R > R_g$ , which levels off to MW-independent regime when  $R < R_g$  (thin black line). The latter regime can be reasonably well described by recent theory.<sup>16,19</sup> In case of adsorbing chains, the same two regimes are present but with  $R_{\text{eff}} = R + R^*$ , where  $R^* \sim R_g$  for  $R > R_g$  (thick blue line), and  $R^*$  defined in some manner by the polymer–NP desorption time in the case of  $R < R_g$  (thin blue line). For the case of strong adsorption and small ( $R < R_g$ ) NPs, nanoparticle diffusion follows polymer chain diffusion at higher MW (thick green line); chain diffusion constant is shown by the dashed red line. (b) The same curves presented as the ratio of diffusion to the classical SE prediction.

literal equilibrium sense when  $R_g > R$ . Certainly the concept of an effective diameter determining NP transport must involve the desorption time scale. But if this concept can be properly formulated, then it opens the door for the construction of a force-based, self-consistent generalized Langevin equation (SCGLE) theory for both repulsive and sticky NPs in polymer melts that unifies the core–shell and vehicle ideas. Efforts in this direction are underway and will be reported in a future publication. Here we simply offer a qualitative discussion of what a general picture might look like per the sketch in Figure 5.

The simplest case is when  $R > R_g$ , where NP diffusion, to leading order, should follow the SE prediction with an effective radius equal to  $R$  for nonadsorbing case and  $\sim R + R_g$  for the strongly adsorbing case. The situation is more complex and interesting when  $R < R_g$ , especially when  $R < d_T/2$ . The behavior of repulsive particles in this regime is well described by current theories,<sup>16,19</sup> including the theory proposed by Rubinstein and co-workers.<sup>15</sup> The NP diffusion can be faster than  $D_{\text{SE}}$  by many orders of magnitude, especially when  $R < d_T/2$  in a strongly entangled melt ( $N \gg N_E$ ).

The situation is less clear for sticky nanoparticles with  $R < R_g$ , where some version of the vehicle mechanism will dominate. It is obvious that when  $\tau_{\text{des}}$  is very long, NP diffusion will be controlled by the dynamics of adsorbed chains (Figure 5). In that case, following paper 1, a small NP with attached chains having  $R_g \gg R$  can be considered roughly as a starlike polymer or related hairy object.<sup>44,45</sup> However, if the desorption time is shorter than the reptation time,  $\tau_{\text{des}} < \tau_{\text{rep}}$ , NP diffusion will become entirely (or nearly so) molecular weight independent at larger MW (Figure 5). In that case, we propose that one can think of the NP diffusion problem as in the nonadsorbing case, but with an *effective size*  $R_{\text{eff}}$  defined by the bare NP radius plus an effective “dynamic layer” of size set by the desorption time. Currently, we cannot provide quantitative estimates of how the desorption time (i.e., activation energy for the chain desorption from the nanoparticle) will define the effective NP size. The desorption time and an effective NP radius are not even considered in another approach developed in ref 15 for nonsticky NPs. Statistical mechanical formulation of this idea is under development. Achieving it would shed light on our observation that the OAPS diffusion coefficient does not reach the expected MW independent regime (Figure 2).

## VII. CONCLUSION

Dynamic light scattering measurements have revealed that the self-diffusion of two chemically similar sticky nanoparticles in PPG melts can be slower and/or faster than the Stokes–Einstein prediction,  $D_{\text{SE}}$ , depending on the size of nanoparticles,  $R$ , relative to the polymer chain size,  $R_g$ . Other time and length scales also matter, especially in the dynamic crossover regime from the core–shell mechanism to the vehicle-like mechanism.<sup>1</sup> Of special importance is the strength of the polymer–NP interactions that defines the segmental desorption time,  $\tau_{\text{des}}$ . At long  $\tau_{\text{des}}$  (strong adsorption), a small NP ( $R \ll R_g$ ) diffuses with the polymer chain. However, if  $\tau_{\text{des}}$  becomes sufficiently short compared to the relevant chain relaxation times, then the NP diffusion constant becomes independent of polymer MW above a threshold value. The threshold is expected to be critically related to  $\tau_{\text{des}}$  but in general is nonuniversal and will also involve other quantities such as the tube diameter, degree of entanglement, and NP diameter. For sufficiently strong attraction and sufficiently small particles compared to the corresponding polymer length and time scales, we expect sticky NP diffusion is ultimately dominated by the “vehicle” mechanism which has various regimes as discussed in detail in paper 1.

On the basis of our combined experimental, theoretical, and simulation results of this work and paper 1, we propose a qualitative general scenario for the diffusion of nanoparticles in a crowded environment with various polymer–NP interactions and for various ratios of  $R$ ,  $R_g$ , and tube diameter. Future studies are required to achieve a deep and predictive quantitative understanding of how these parameters determine the nanoparticle diffusion coefficient. But our present initial effort is useful for understanding various dynamical issues in polymer nanocomposite materials and also some biological systems as well.

## ■ AUTHOR INFORMATION

### Corresponding Authors

\*E-mail [sokolov@utk.edu](mailto:sokolov@utk.edu) (A.P.S.).

\*E-mail [bocharovav@ornl.gov](mailto:bocharovav@ornl.gov) (V.B.).

### ORCID

Bobby Carroll: 0000-0002-0536-9734

Vera Bocharova: 0000-0003-4270-3866

Jan-Michael Y. Carrillo: 0000-0001-8774-697X

Shiwang Cheng: 0000-0001-7396-4407

Bobby G. Sumpter: 0000-0001-6341-0355

## Notes

The authors declare no competing financial interest.

## ACKNOWLEDGMENTS

This work was supported by the U.S. Department of Energy, Office of Science, Basic Energy Sciences, Materials Science and Engineering Division. Simulations were performed at the Center for Nanophase Materials Sciences, which is a US Department of Energy Office of Science User Facility. This research also used resources of the Oak Ridge Leadership Computing Facility at Oak Ridge National Laboratory, which is supported by the Office of Science of the Department of Energy under Contract DE-AC05-00OR22725.

## REFERENCES

- (1) Yamamoto, U.; Carrillo, J.-M.; Bocharova, V.; Sokolov, A. P.; Sumpter, B. G.; Schweizer, K. S. Theory and simulation of attractive nanoparticle transport in polymer melts. *Macromolecules* **2018**, DOI: 10.1021/acs.macromol.7b02694.
- (2) Tuteja, A.; Mackay, M. E.; Narayanan, S.; Asokan, S.; Wong, M. S. Breakdown of the continuum Stokes-Einstein relation for nanoparticle diffusion. *Nano Lett.* **2007**, *7*, 1276.
- (3) Grabowski, C. A.; Adhikary, B.; Mukhopadhyay, A. Dynamic of gold nanoparticles in a polymer melt. *Appl. Phys. Lett.* **2009**, *94*, 021903.
- (4) Kohli, I.; Mukhopadhyay, A. Diffusion of nanoparticles in semidilute polymer solutions: effect of different length scales. *Macromolecules* **2012**, *45*, 6143–6149.
- (5) Guo, H.; Bourret, G.; Lennox, R. B.; Sutton, M.; Harden, J. L.; Leheny, R. L. Entanglement-controlled subdiffusion of nanoparticles within concentrated polymer solutions. *Phys. Rev. Lett.* **2012**, *109*, 055901.
- (6) Alam, S.; Mukhopadhyay, A. Translational and rotational diffusions of nanorods within semidilute and entangled polymer solutions. *Macromolecules* **2014**, *47*, 6919–6924.
- (7) Chapman, C. D.; Lee, K.; Henze, D.; Smith, D. E.; Robertson-Anderson, R. M. Onset of non-continuum effects in microrheology of entangled polymer solutions. *Macromolecules* **2014**, *47*, 1181–1186.
- (8) Grabowski, C. A.; Mukhopadhyay, A. Size effect of nanoparticle diffusion in a polymer melt. *Macromolecules* **2014**, *47*, 7238–7242.
- (9) Lin, C.-C.; Parrish, E.; Composto, R. J. Macromolecule and particle dynamics in confined media. *Macromolecules* **2016**, *49*, 5755.
- (10) Lungova, M.; Krutyeva, M.; Pyckhout-Hintzen, W.; Wischniewski, A.; Monkenbusch, M.; Allgaier, J.; Ohl, M.; Sharp, M.; Richter, D. Nanoscale motion of soft nanoparticles in unentangled and entangled polymer matrices. *Phys. Rev. Lett.* **2016**, *117*, 147803.
- (11) Maldonado-Camargo, L.; Rinaldi, C. Breakdown of the Stokes-Einstein relation for the rotational diffusivity of polymer grafted nanoparticles in polymer melts. *Nano Lett.* **2016**, *16*, 6767–6773.
- (12) Mangal, R.; Srivastava, S.; Narayanan, S.; Archer, L. A. Size-dependent particle dynamics in entangled polymer nanocomposites. *Langmuir* **2016**, *32*, 596–603.
- (13) Senses, E.; Narayanan, S.; Mao, Y.; Faraone, A. Nanoscale particle motion in attractive polymer nanocomposites. *Phys. Rev. Lett.* **2017**, *119*, 237801.
- (14) Brochard-Wyart, F.; de Gennes, P. G. Viscosity at small scales in polymer melts. *Eur. Phys. J. E: Soft Matter Biol. Phys.* **2000**, *1*, 93.
- (15) Cai, L.-H.; Panyukov, S.; Rubinstein, M. Mobility of nonsticky nanoparticles in polymer liquids. *Macromolecules* **2011**, *44*, 7853–7863.
- (16) Yamamoto, U.; Schweizer, K. S. Theory of nanoparticle diffusion in unentangled and entangled polymer melts. *J. Chem. Phys.* **2011**, *135*, 224902.
- (17) Ganesan, V.; Jayaraman, A. Theory and simulation studies of effective interactions, phase behavior and morphology in polymer nanocomposites. *Soft Matter* **2014**, *10*, 13–38.
- (18) Cai, L.-H.; Panyukov, S.; Rubinstein, M. Hopping diffusion of nanoparticles in polymer matrices. *Macromolecules* **2015**, *48*, 847–862.
- (19) Yamamoto, U.; Schweizer, K. S. Microscopic theory of the long-time diffusivity and intermediate-time anomalous transport of a nanoparticle in polymer melts. *Macromolecules* **2015**, *48*, 152–163.
- (20) Dell, E. Z.; Schweizer, K. S. Theory of localization and activated hopping of nanoparticles in cross-linked networks and entangled polymer melts. *Macromolecules* **2014**, *47*, 405–414.
- (21) Liu, J.; Cao, D.; Zhang, L. Molecular dynamics study on nanoparticle diffusion in polymer melts: a test of the Stokes-Einstein law. *J. Phys. Chem. C* **2008**, *112*, 6653–6661.
- (22) Kalathi, J. T.; Yamamoto, U.; Schweizer, K. S.; Grest, G. S.; Kumar, S. K. Nanoparticle diffusion in polymer nanocomposites. *Phys. Rev. Lett.* **2014**, *112*, 108301.
- (23) Vrentas, J. S.; Duda, J. L.; Ling, H. C. Free volume theories for self-diffusion in polymer-solvent systems. I. Conceptual differences in theories. *J. Polym. Sci., Polym. Phys. Ed.* **1985**, *23*, 275.
- (24) Cheng, S.; Carroll, B.; Bocharova, V.; Carrillo, J.-M.; Sumpter, B.; Sokolov, A. *J. Chem. Phys.* **2017**, *146*, 203201.
- (25) Liang, H.-W.; Wang, L.; Chen, P.-Y.; Lin, H.-T.; Chen, L.-F.; He, D.; Yu, S.-H. Carbonaceous nanofiber membranes for selective filtration and separation of nanoparticles. *Adv. Mater.* **2010**, *22*, 4691–4695.
- (26) Pradeep, T.; Anshup. Noble metal nanoparticles for water purification: a critical review. *Thin Solid Films* **2009**, *517*, 6441–6478.
- (27) Daniel, M.-C.; Astruc, D. Gold nanoparticles: assembly, supramolecular chemistry, quantum-size-related properties, and applications toward biology, catalysis, and nanotechnology. *Chem. Rev.* **2004**, *104*, 293–346.
- (28) Lavan, D. A.; McGuire, T.; Langer, R. Small-scale systems for in vivo drug delivery. *Nat. Biotechnol.* **2003**, *21*, 1184.
- (29) Mora-Huertas, C.; Fessi, H.; Elaissari, A. Polymer-based nanocapsules for drug delivery. *Int. J. Pharm.* **2010**, *385*, 113.
- (30) Wang, Y.; Li, C.; Pielak, G. J. Effects of proteins on protein diffusion. *J. Am. Chem. Soc.* **2010**, *132*, 9392.
- (31) Wilkins, D. K.; Grimshaw, S. B.; Receveur, V.; Dobson, C. M.; Jones, J. A.; Smith, L. J. Hydrodynamic radii of native and denatured proteins measured by pulse field gradient NMR techniques. *Biochemistry* **1999**, *38*, 16424.
- (32) Zorrilla, S.; Hink, M. A.; Visser, A. J.; Lillo, M. P. Translational and rotational motions of proteins in a protein crowded environment. *Biophys. Chem.* **2007**, *125*, 298.
- (33) Rubinstein, M.; Colby, R. H. *Polymer Physics*; Oxford University Press: Oxford, 2003.
- (34) Banks, D. S.; Fradin, C. Anomalous diffusion of proteins due to molecular crowding. *Biophys. J.* **2005**, *89*, 2960.
- (35) Vagias, A.; Raccis, R.; Koynov, K.; Jonas, U.; Butt, H.-J.; Fytas, G.; Kosovan, P.; Lenz, O.; Holm, C. Complex tracer diffusion dynamics in polymer solutions. *Phys. Rev. Lett.* **2013**, *111*, 088301.
- (36) Omari, R. A.; Aneese, A. M.; Grabowski, C. A.; Mukhopadhyay, A. Diffusion of nanoparticles in semidilute and entangled polymer solutions. *J. Phys. Chem. B* **2009**, *113*, 8449.
- (37) Griffin, P. J.; Bocharova, V.; Middleton, L. R.; Composto, R. J.; Clarke, N.; Schweizer, K. S.; Winey, K. I. Influence of the bound polymer layer on nanoparticle diffusion in polymer melts. *ACS Macro Lett.* **2016**, *5*, 1141.
- (38) Fetters, L. J.; Lohse, D. J.; Richter, D.; Witten, T. A.; Zirkel, A. Connection between polymer molecular weight, density, chain dimensions, and melt viscoelastic properties. *Macromolecules* **1994**, *27*, 4639.
- (39) Gainaru, C.; Hiller, W.; Bohmer, R. Dielectric study of oligo- and poly(propylene glycol). *Macromolecules* **2010**, *43*, 1907.
- (40) Kresse, G.; Furthmüller, J. Efficiency of ab-initio total energy calculations for metals and semiconductors using a plane-wave basis set. *Comput. Mater. Sci.* **1996**, *6*, 15–50.

- (41) Perdew, J. P.; Burke, K.; Ernzerhof, M. Generalized gradient approximation made simple. *Phys. Rev. Lett.* **1996**, *77*, 3865–3868.
- (42) Lee, K.; Murray, E. D.; Kong, L.; Lundqvist, B. I.; Langreth, D. C. Higher-accuracy van der Waals density functional. *Phys. Rev. B: Condens. Matter Mater. Phys.* **2010**, *82*, 081101.
- (43) Cheng, S.; Xie, S.-J.; Carrillo, J.-M. Y.; Carroll, B.; Martin, H.; Cao, P.-F.; Dadmun, M. D.; Sumpter, B. G.; Novikov, V. N.; Schweizer, K. S.; Sokolov, A. P. Big effect of small nanoparticles: a shift in paradigm for polymer nanocomposites. *ACS Nano* **2017**, *11*, 752.
- (44) Doi, M. Relaxation spectra of nonlinear polymers. *Polym. J.* **1974**, *6*, 108.
- (45) Daoud, M.; de Gennes, P.-G. Some remarks on the dynamics of polymer melts. *J. Polym. Sci., Polym. Phys. Ed.* **1979**, *17*, 1971.